0026-895X/02/6106-1423–1434$7.00
MOLECULAR PHARMACOLOGY
Copyright © 2002 The American Society for Pharmacology and Experimental Therapeutics
Mol Pharmacol 61:1423–1434, 2002

Vol. 61, No. 6
1368/982054
Printed in U.S.A.

The Muscarinic Acetylcholine Receptor-Stimulated Increase in Aquaporin-5 Levels in the Apical Plasma Membrane in Rat Parotid Acinar Cells Is Coupled with Activation of Nitric Oxide/cGMP Signal Transduction

YASUKO ISHIKAWA, HIROKAZU IIDA, and HAJIME ISHIDA

Department of Pharmacology, Tokushima University School of Dentistry, Tokushima, Japan

Received September 20, 2001; accepted February 15, 2002

This article is available online at http://molpharm.aspetjournals.org

ABSTRACT

The present study investigated the role of nitric oxide (NO)/cGMP signal transduction in the M_3 muscarinic acetylcholine receptor (mAChR)-stimulated increase in aquaporin-5 (AQP5) levels in the apical plasma membrane (APM) of rat parotid glands. Pretreatment of rat parotid tissue with the NO scavenger 2-(4carboxyphenyl)-4,4,5,5-tetramethyl-imidazoline-1-oxyl-3-oxide potassium inhibited both acetylcholine (ACh)- and pilocarpine-induced increases in AQP5 in the APM. NO donors [3-morpholinosydnonimine (SIN-1) and (*S*)-nitroso-*N*-acetylpenicillamine (SNAP)] mimicked the effects of mAChR agonists. A selective protein kinase G inhibitor [(9*S*,10*R*,12*R*)-2,3,9,10,11,12-hexahydro-10-methoxy-2,9-dimethyl-1-oxo-9,12-epoxy-1H-diindolo-[1,2,3-*fg*-3′,2′,1′-*kl*]pyrrolo[3,4-*i*][1,6]benzodiazocine-10-carboxylic acid methyl ester (KT5823)] and an NO synthase inhibitor (N^6-imminoethyl-L-lysine) blocked SIN-1- and SNAP-induced increases in AQP5 in the APM. A calmodulin kinase II inhibitor [(8)-5-isoquinolinesulfonic acid, 4-[2-(5-isoquinolinyl-sulfonyl)methylamino]-3-oxo-(4-phenyl-1-piperazinyl)-propyl]phenyl ester (KN-62)] decreased the pilocarpine-induced increase of AQP5 in the APM. Using diaminofluorescinein-2 diacetate, enhanced NO synthase activity was detected in isolated parotid acinar cells after ACh-treatment. Treatment with dibutyryl cGMP, but not dibutyryl cAMP, induced an increase in AQP5 levels in the APM. BAPTA-AM inhibited the cGMP-induced increase in AQP5 in the APM. Pretreatment of the tissues with a myosin light chain kinase inhibitor [(5-chloronaphthalene-1-sulfonyl)-1H-hexahydro-1,4-diazepine (ML-9)] inhibited a mAChR-stimulated increase in AQP5 levels in the APM. Although there was a significant ACh-induced increase in AQP5 in the APM in the absence of extracellular Ca^{2+}, the maximal effect of ACh on the AQP5 levels in the APM occurred in the presence of extracellular Ca^{2+}. These results suggest that NO/cGMP signal transduction has a crucial role in Ca^{2+} homeostasis in the mAChR-stimulated increase in AQP5 levels in the APM of rat parotid glands.

Several aquaporins (AQPs), which form water channels that selectively transport water across the plasma membrane, have been cloned from a variety of mammalian tissues (King and Agre, 1996). In the gastrointestinal tract, more than seven AQPs are known to be expressed: AQP1 in intrahepatic cholangiocytes; AQP4 in gastric parietal cells; AQP3 and AQP4 in colonic surface epithelium; AQP5 in salivary glands; AQP7 in small intestine; AQP8 in liver, pancreas, colon, and salivary glands; and AQP9 in liver (Ma and Verkman, 1999). AQP5 was cloned from the rat submandibular gland (Raina et al., 1995). The nucleotide sequence of AQP5 reveals 45 and 63% homology with AQP1 and AQP2, respectively (Raina et al., 1995). Salivary fluid secretion is defective in transgenic mice lacking AQP5, indicating that AQP5 is important in salivary gland function (Ma et al., 1999; Krane et al., 2001). The sympathetic and parasympathetic nerves in rat parotid glands regulate the role of AQP5. Acetylcholine (ACh) and epinephrine acting at M_3 muscarinic acetylcholine receptors (mAChR) and α_1-adrenoceptors, respectively, in-

This work was supported in part by a grant-in-aid for scientific research from the Ministry of Education, Culture, Sports, Science, and Technology of Japan.

ABBREVIATIONS: AQP, aquaporin; ACh, acetylcholine; mAChR, muscarinic acetylcholine receptor; APM, apical plasma membrane; SNI-2011, cevimeline hydrochloride; PLC, phospholipase C; IP_3, inositol 1,4,5-trisphosphate; DAG, 1,2-diacylglycerol; PKC, protein kinase C; CaM, calmodulin; MLCK, myosin light chain kinase; NOS, nitric-oxide synthase; GC, guanylate cyclase; NO, nitric oxide; PKG, protein kinase G; BAPTA-AM, 1,2-bis(2-aminophenoxy)ethane-*N*,*N*,*N*′,*N*′-tetraacetic acid-acetoxymethyl ester; Carboxy-PTIO, 2-(4carboxyphenyl)-4,4,5,5-tetramethyl-imidazoline-1-oxyl-3-oxide potassium; IBMX, 3-isobutyl-1-methylxanthine; SIN-1, 3-morpholinosydnonimine; SNAP, (*S*)-nitroso-*N*-acetylpenicillamine; KN-62; (8)-5-isoquinolinesulfonic acid, 4-[2-(5-isoquinolinyl-sulfonyl)methylamino]-3-oxo-(4-phenyl-1-piperazinyl)-propyl]phenyl ester; ML9, (5-chloronaphthalene-1-sulfonyl)-1H-hexahydro-1,4-diazepine; DAF-2/DA, diaminofluorescinein-2 diacetate; KRT, Krebs-Ringer-Tris; PAGE, polyacrylamide gel electrophoresis; DTT, dithiothreitol; MOPS, 3-(*N*-morpholino)propanesulfonic acid; KT5823, (9*S*,10*R*,12*R*)-2,3,9,10,11,12-hexahydro-10-methoxy-2,9-dimethyl-1-oxo-9,12-epoxy-1H-diindolo-[1,2,3-*fg*-3′,2′,1′-*kl*]pyrrolo[3,4-*i*][1,6]benzodiazocine-10-carboxylic acid methyl ester; dbcGMP, dibutyryl cGMP.

duce a rapid increase in AQP5 levels in the APM by increasing the cytosolic concentration of Ca^{2+} ($[Ca^{2+}]_i$) (Ishikawa et al., 1998, 1999). In contrast, SNI-2011 and pilocarpine induce a long-lasting increase in AQP5 levels in the APM in rat parotid glands (Ishikawa et al., 2000). The site of action of Ca^{2+} for the increase in AQP5 levels in the APM of rat parotid cells, however, is not known.

M_3 mAChRs trigger similar signal transduction pathways that involve the heterotrimeric G protein Gq-mediated activation of phospholipase C (PLC)-*β*, which results in the generation of inositol 1,4,5-trisphosphate (IP_3) and 1,2-diacylglycerol (DAG). IP_3 then induces an increase in $[Ca^{2+}]_i$, whereas DAG activates protein kinase C (PKC) (Putney, 1986; Baum, 1993). The ryanodine receptor type III has also been identified in microsomal membranes of mouse parotid acini and has an important role in Ca^{2+} homeostasis (Dijulio et al., 1997). In Ca^{2+}-mediated intracellular signal transduction mechanisms, an increase in $[Ca^{2+}]_i$ has an important role in the activation of Ca^{2+}/calmodulin (CaM)-dependent proteins, such as CaM kinases, myosin light chain kinase (MLCK), and nitric-oxide synthase (NOS). CaM kinase II is a multifunctional enzyme that is required for both granule mobilization under stimulation conditions and maintenance of secretory capacity under control conditions in pancreatic *β*-cells (Gromada et al., 1999). MLCK seems to be involved in Ca^{2+}-dependent secretion of insulin (Niwa et al., 1998), renin (Kim et al., 1998), and catecholamines (Kumakura et al., 1994). The roles of CaM kinase II and MLCK on salivary secretion, however, are not known. Through the stimulation of guanylyl cyclase (GC), NO increases cGMP formation (Moncada et al., 1991; Lucas et al., 2000).

Recent studies have focused on the mechanisms underlying the regulation of AQPs to clarify the molecular basis of water movement across biologic membranes. AQP1 has a cyclic nucleotide binding domain in the C terminus and is activated by direct binding of cGMP (Anthony et al., 2000). Protein kinase G (PKG), which is activated by cGMP, phosphorylates AQP2 on the C-terminal residue and increases the insertion of AQP2 into renal epithelial cells (Bouley et al., 2000). Whether these Ca^{2+}/CaM-dependent enzymes are involved in the mechanisms underlying the increase of AQP5 in the APM of rat parotid cells, however, remains unknown.

The aim of this study was to investigate the possible roles of CaM kinase II, NOS, MLCK, and PKG in ACh- and pilocarpine-induced increases in AQP5 levels in the APM of rat parotid cells. We report that endogenous NOS is present in rat parotid acinar cells and that activation of NOS together with CaM kinase II, MLCK, and PKG is coupled with ACh- and pilocarpine-induced increases in AQP5 levels in the APM of the cells.

Experimental Procedures

Materials. BAPTA-AM, 2-(4carboxyphenyl)-4,4,5,5-tetramethylimidazoline-1-oxyl-3-oxide potassium (Carboxy-PTIO), 3-isobutyl-1-methylxanthine (IBMX), and RPMI 1640 medium were obtained from Sigma Chemical Co. (St. Louis, MO). 3-Morpholinosydnonimine (SIN-1), [(*S*)-nitroso-*N*-acetylpenicillamine], N^6-imminoethyl-L-lysine (L-NIL), (8)-5-isoquinolinesulfonic acid, 4-[2-(5-isoquinolinylsulfonyl)methylamino]-3-oxo-(4-phenyl-1-piperazinyl)-propyl]phenyl ester (KN-62) were obtained from Funakoshi Co. (Tokyo, Japan). 1-(5-chloronaphthalene-1-sulfonyl)-1H-hexahydro-1,4-diazepine (ML-9) was obtained from Biomol Research Laboratories, Inc. (Plymouth Meeting, PA). Diaminofluorescinein-2 diacetate (DAF-2/DA) was obtained from Daiichi Pure Chemicals Co., Ltd. (Tokyo, Japan). Collagenase was obtained from Worthington Biochemical (Lakewood, NJ).

Preparation and Incubation of Rat Parotid Tissue. Male Wistar rats (8 weeks old) were provided with laboratory chow (MF; Oriental Yeast, Tokyo, Japan) and water ad libitum and were maintained in a temperature-controlled environment (22 ± 2°C) with a 12-h light/dark cycle (lights on at 6:00 AM). The Animal Care committee of Tokushima University Dental School approved all procedures. Rats were killed by a blow to the head, and the parotid glands were rapidly removed and transferred to ice-cold Krebs-Ringer-Tris (KRT) solution [120 mM NaCl, 4.8 mM KCl, 1.2 mM KH_2PO_4, 1.2 mM $MgSO_4$, 1.0 mM $CaCl_2$, 16 mM Tris-HCl, pH 7.4, and 5 mM glucose] that had been aerated with O_2 gas. Tissue slices (0.4 mm thick) were prepared from the parotid glands using a McIlwain Tissue Chopper (Mickle Laboratory Engineering, Surrey, UK) and equilibrated with the KRT solution for 20 min at 37°C with shaking, as described previously (Hata et al., 1983). The slices (wet weight, 300 mg) were then incubated at 37°C in 10 ml of KRT solution in the presence or absence of ACh or other agents as indicated.

Preparation of APM Fraction of Rat Parotid Tissue. The APM fraction was prepared from rat parotid glands with a slight modification as described previously (Ishikawa et al., 1998). Briefly, tissue slices were homogenized with a glass homogenizer and Teflon pestle in 20 volumes of 5 mM HEPES buffer, pH 7.5, containing 50 mM mannitol and 0.25 mM $MgCl_2$, and the homogenate was filtered through a single layer of nylon bolting cloth (150 mesh). The filtrate was subjected to differential centrifugation, and the pellet obtained after centrifugation at 35,000*g* for 30 min was suspended in the buffer described above. After the addition of 1 M $MgCl_2$ to give a final concentration of 10 mM, the suspension was incubated on ice for 30 min with stirring and then centrifuged at 3,000*g* for 15 min. The resultant pellet was saved as fraction 1 and the supernatant was again centrifuged at 35,000*g* for 30 min. The new pellet was saved as fraction 2, and the supernatant was centrifuged at 200,000*g* for 1 h to yield a pellet that was saved as fraction 3. γ-Glutamyltranspeptidase was used as a marker for the APM (Paul et al., 1992) and K^+-stimulated *p*-nitrophenyl phosphatase was used as a marker for the basolateral plasma membrane (Turner et al., 1986) as described previously. The specific activity of γ-glutamyltranspeptidase for fractions 1, 2, and 3 was 375 ± 5.6, 18.3 ± 0.9, and 28.5 ± 2.7 nmol/min/mg of protein, respectively. The specific activity of K^+-stimulated *p*-nitrophenyl phosphatase for fractions 1, 2, and 3 was 36.9 ± 3.6, 11.1 ± 1.2, and 61.8 ± 4.3 nmol/min/mg of protein, respectively. Fractions 1, 2, and 3 were enriched in the APM, intracellular membrane, and basolateral plasma membrane, respectively, consistent with the results of Paul et al. (1992).

Preparation of Antibodies to AQP5. Rabbit polyclonal antibodies to AQP5 were generated in response to a synthetic peptide (KGTYEPEEDWEDHREERKKTI), which corresponded to the deduced carboxyl-terminal amino acid sequence of AQP5 (Raina et al., 1995).

Immunoblot Analysis. The APM fraction was treated with solubilizing buffer (Laemmli, 1970) and subjected to SDS-polyacrylamide gel electrophoresis (PAGE) on a 12.5% gel. After PAGE, the separated proteins were transferred electrophoretically from the unstained gel to a nitrocellulose membrane (Hybond ECL; Amersham Biosciences, Little Chalfont, Buckinghamshire, UK) using a Trans-Blot apparatus (Bio-Rad, Hercules, CA). The blots were probed with antibodies to AQP5 (1:1500 dilution). Immune complexes were detected with horseradish peroxidase-conjugated secondary antibodies and enhanced chemiluminescence reagents (Amersham Biosciences).

Purification of AQP5. Parotid tissues were solubilized in 1% Triton X-100, 20 mM Tris-HCl buffer, pH 7.4, 125 mM NaCl, 1 mM $MgCl_2$, 1 mM $CaCl_2$, 10 μg/ml aprotinin, and 10 μg/ml leupeptin at 4°C for 1 h with gentle stirring, and then centrifuged at 9000 *g* for 10 min at 4°C to remove nonsolubilized materials. The resulting supernatants were incubated with anti-AQP5 antibody, diluted 1:20 in the

same buffer for 12 h, and applied to a Protein A-Sepharose CL-4B column (1.5 × 2.0 cm; Pharmacia Fine Chemicals, Uppsala, Sweden) pre-equilibrated with 20 mM sodium phosphate buffer, pH 7.0. The immune complex was eluted at a flow rate of 0.2 ml/min with 100 mM glycine-HCl buffer, pH 2.7. After dialysis against H_2O, the eluate was concentrated and dissolved, without heating, in solubilizing buffer. The solubilized AQP5 was subjected to SDS-PAGE in 12.5% linear polyacrylamide gels and subjected to immunoblot.

Determination of NOS Activity in Parotid Acinar Cells. Rat parotid acinar cells were isolated by collagenase and hyaluronidase digestion as described previously (Ishikawa et al., 2000) and were incubated in RPM1 1640 medium with 10 μM DAF-2/DA for 30 min at 37°C, which was aerated with 95% O_2/5% CO_2 at pH 7.4. Acinar cells were washed and resuspended in a HEPES-buffered Krebs-Ringer-bicarbonate medium containing 118.46 mM NaCl, 4.74 mM KCl, 1.18 mM KH_2PO_4, 1.00 mM $CaCl_2$, 1.18 mM $MgSO_4$, 24.88 mM $NaHCO_3$, and 5 mM HEPES, pH 7.4, and then suspended to measure NOS activity by fluorescence study with DAF-2/DA as described by Tritsaris et al. (2000). The cells were gently stirred in a cuvette maintained at 37°C with or without ACh and other agents as indicated. Changes in fluorescence, which were generated by reaction of DAF-2 with NO, were monitored with a fluorescence spectrometer (F-4000: Hitachi, Tokyo, Japan). The experiments were performed with an excitation wavelength of 495 nm (5-nm bandwidth) and an emission wavelength of 515 nm (5-nm bandwidth). Agents were added to the cuvette to give the final concentrations shown in Fig. 6.

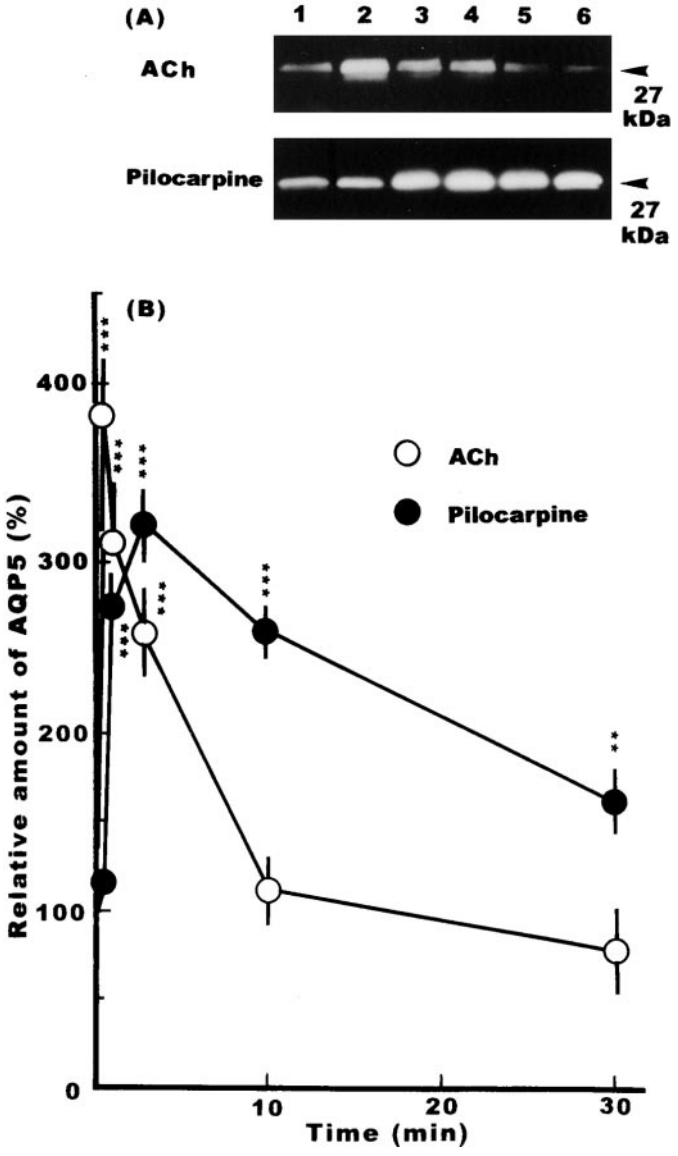

Fig. 1. Time course for the effect of ACh and pilocarpine on AQP5 levels in the APM of rat parotid glands. A, rat parotid tissue slices were incubated in the presence of 10 μM ACh plus 1 μM eserine or 10 μM pilocarpine for 0, 0.25, 1, 3, 10, or 30 min (corresponding to lanes 1–6, respectively, in the inset) at 37°C, after which APM (5 μg of protein) fractions were prepared and subjected to immunoblot analysis with antibodies to AQP5. The position of the 27-kDa immunoreactive protein is indicated. B, immunoblots were subjected to densitometric analysis, and the amount of AQP5 in APM, based on the intensity of the chemiluminescence signal, was expressed as a percentage of the value for control tissue. 10 μM ACh plus 1 μM eserine (○) or 10 μM pilocarpine (●). Data are means ± S.E. of five independent experiments. ★★★, $p < 0.001$; ★★, $p < 0.01$ versus the value for control cells.

Measurement of $[Ca^{2+}]_i$ in Parotid Acinar Cells. Parotid acinar cells, prepared by collagenase/hyaluronidase digestion, were subjected to measurement of $[Ca^{2+}]_i$ according to fluorescence study with fura-2/AM. The cells were gently stirred in the cuvette maintained at 37°C during the assay. Changes in fura-2 fluorescence were monitored with a fluorescence spectrometer (F-4000; Hitachi, Tokyo, Japan). Excitation was performed at 340 and 380 nm, and emission was measured at 510 nm. The $[Ca^{2+}]_i$ was calculated from the ratio (340/380 nm) of fluorescence intensities after subtraction of autofluorescence, as described previously (Ishikawa et al., 2000) .

Assay of CaM Kinase II, PKG, and MLCK Activities in Rat Parotid Tissue Slices. After incubating under experimental conditions, the parotid tissue slices were rapidly frozen at −80°C. For measurement of CaM kinase II activity, the frozen slices were homogenized in a solution containing 20 mM Tris-HCl, pH 8.0, 2 mM EDTA, 2 mM EGTA, 20 μg/ml soybean trypsin inhibitor, 10 μg/ml aprotinin, 5 μg/ml leupeptin, 2 mM dithiothreitol (DTT), 25 mM benzamidine, and 1 mM phenylmethylsulfonyl fluoride. The homogenate was centrifuged at 350*g* for 5 min, and the resulting supernatant was diluted with a solution containing 50 mM Tris-HCl, pH 7.5, 10 mM $MgCl_2$, 0.1 mM DTT, and 0.1 mg/ml bovine serum albumin before assay of CaM kinase II activity with a specific assay kit.

For measurement of PKG activity, the frozen tissue slices were homogenized in a solution composed of 20 mM HEPES, pH 7.5, 10 mM EGTA, 40 mM β-glycerophosphate, 1% Nonidet P-40, 25 mM $MgCl_2$, 2 mM sodium orthovanadate, 140 mM NaCl, 1 mM DTT, 1 mM Pefabloc (Pentapharm Ltd., Basel, Switzerland), 10 μg/ml aprotinin, and 10 μg/ml leupeptin. The homogenate was centrifuged for 15 min at 5,000*g* and the resultant supernatant was assayed for PKG activity with a specific kit. In brief, 100 μl of the supernatant was added to 50 μl of assay mixture containing 20 mM Tris-HCl, pH 7.4, 200 μM ATP, 100 μM BPDEtide, 20 mM $MgCl_2$, 100 μM IBMX, 1 μM (6–22)amide, and 0.5 μCi of [γ-^{32}P]ATP. After incubation for 10 min at 30°C, the incorporation of ^{32}P into BPDEtide was determined.

For measurement of MLCK activity, the parotid tissue slices were homogenized in a solution containing 20 mM MOPS, pH 7.0, 1% Nonidet P-40, 0.5 mM EGTA, 50 mM $MgCl_2$, 10% glycerol, 10 mM DTT, 10 μg/ml soybean trypsin inhibitor, 20 μg/ml aprotinin, 10 μg/ml leupeptin, 25 mM benzamidine, and 1 mM phenylmethylsulfonyl fluoride. The homogenate was centrifuged for 2 min at 7000*g*, and the resultant supernatant was determined in reactions having 50 mM MOPS, pH 7.0, 10 mM $Mg(CH_3COO)_2$, 1 mM DTT, 0.2 mM $CaCl_2$ or 2 mM EGTA, 1 mM [γ-^{32}P]ATP, 1 μM calmodulin, and 26.5 μM myosin. After incubation for 10 min at 30°C, a trichloroacetic acid/$Na_4P_2O_7$ solution to give final concentrations (w/v) of 10% trichloroacetic acid and 2% $Na_4P_2O_7$. The precipitated protein was trapped by filter on a Millipore filtration apparatus (Millipore, Bedford, MA). After washing with 5% trichloroacetic acid and 2% $Na_4P_2O_7$, the filter was counted for radioactivity.

cGMP Assay. The amount of cGMP in the tissues was measured using a radioimmunoassay kit (Yamasa Shoyu, Tokyo, Japan).

Statistical Analysis. Data are presented as means ± S.E. and were analyzed for statistical significance with Student's *t* test or

analysis of variance at all time points. A P value of less than 0.05 was considered statistically significant.

Results

Effect of ACh and Pilocarpine on AQP5 Levels in the APM in Rat Parotid Tissue. Rat parotid tissue slices were incubated for 0.25, 1, 3, 10, and 30 min at 37°C with 10 μM ACh plus 1 μM eserine or 10 μM pilocarpine to determine whether these agents increased AQP5 levels in the APM (Fig. 1). Eserine alone (1 μM), which inhibits cholinesterase activity, did not affect the amount of AQP5 in the APM (Fig. 2A, lane 6). In the following experiments, 1 μM eserine was used with ACh. The tissues were then immediately frozen to stop the reaction before homogenization and preparation of membrane fractions. Immunoblot analysis with antibodies to AQP5 revealed that ACh induced a marked increase in AQP5 levels in the APM with the maximum (381 ± 31% of control) at 0.25 min and pilocarpine induced a marked increase with a maximum (320 ± 19% of control) at 3 min (Fig. 1). Although the total amount of AQP5 in the parotid tissues stimulated by ACh was the same as that in the nonstimulated tissues, treatment of the tissues with either ACh or pilocarpine increased AQP5 levels in the APM in rat parotid glands.

The ACh- or pilocarpine-induced increase in the amount of AQP5 in the APM was concentration-dependent with a maximum at 1 μM ACh (Fig. 2A) or 10 μM pilocarpine (Fig. 2B), respectively. The amount of AQP5 in the APM of parotid tissues incubated with 10 μM ACh or 10 μM pilocarpine was not significantly different from that in parotid tissues incubated with 1 μM ACh or 10 μM pilocarpine, respectively. In the following experiments, 10 μM ACh or 10 μM pilocarpine was used.

As shown in Fig. 2C, AQP5 was purified using protein A Sepharose CL-4B and subjected to Western blotting. The antibodies to AQP5 recognized a single protein band with a mobility corresponding to a molecular mass of 27 kDa (Fig. 2C, lane 1). Detection of this protein was prevented by preadsorption of the antibodies to AQP5 with excess immunizing peptide (Fig. 2C, lane 2).

Effect of NO Scavenger on Both ACh- and Pilocarpine-Induced Increases of AQP5 in the APM. In parotid glands, the stimulation of M_3 mAChRs with their agonists generates IP_3 and DAG through the stimulation of Gq protein and PLC. IP_3 is then involved in the subsequent elevation of $[Ca^{2+}]_i$ (Putney, 1986; Baum, 1993). The rise in $[Ca^{2+}]_i$ has a key role in both ACh- and SNI-2011–induced increases in AQP5 levels in the APM (Ishikawa et al., 2000). Recently, generation and release of NO was recognized as an important second messenger pathway when an elevation of $[Ca^{2+}]_i$ induced the activation of the CaM-dependent enzyme NOS (Moncada et al., 1991; Bredt and Snyder, 1994). The NO scavenger carboxy-PTIO was used to investigate the effect of NO on AQP5 levels in the APM. Pretreatment of parotid tissues for 10 min with 10 μM carboxy-PTIO inhibited ACh- and pilocarpine-induced increases in AQP5 in the APM (Fig. 3), indicating that NO contributes to the increase of AQP5 in the APM in rat parotid tissues.

Effect of NO on AQP5 Levels in the APM. To further examine the effect of NO on the increase of AQP5 in the APM, we investigated the effects of the exogenous NO donors SIN-1, which spontaneously liberates NO (Kankaanranta et al., 1997), and SNAP, which forms (*S*)-nitrosothiol (Jansen et al., 1992). Exposure of parotid tissue for 10 min to 1 mM SIN-1 or 1 mM SNAP in the presence of 0.5 mM IBMX, which inhibited cGMP phosphodiesterase activity, induced 10- and 15-fold increases, respectively, in the concentration of cGMP (none, 26.7 ± 2.3; SIN-1, 245.9 ± 2.9; SNAP, 395.2 ± 2.8

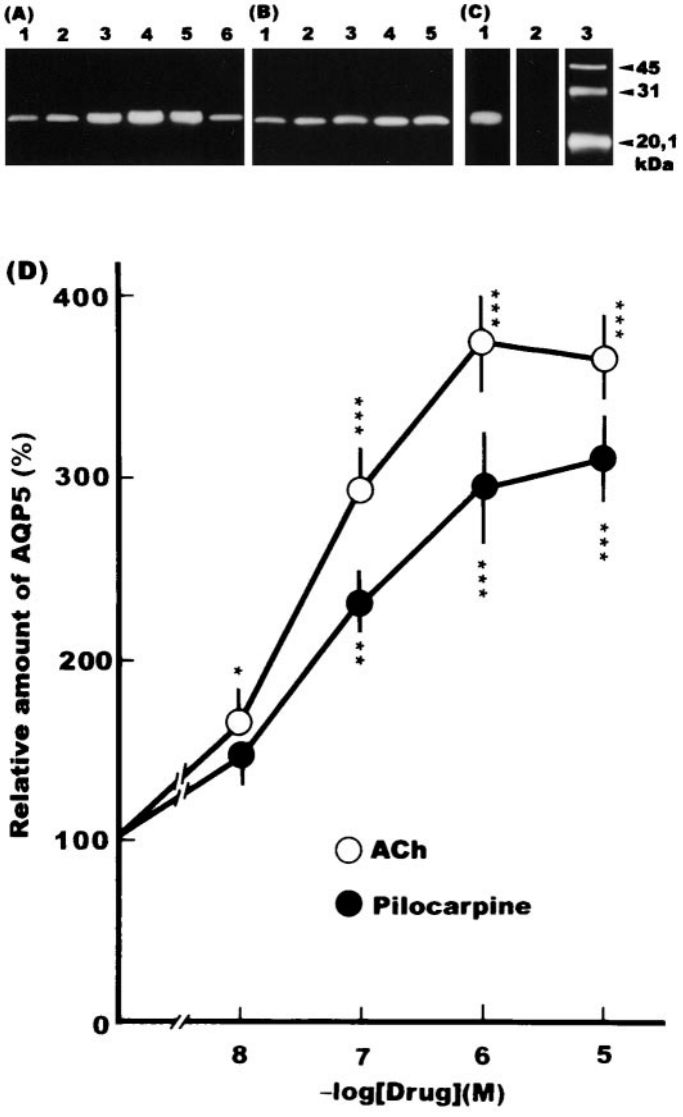

Fig. 2. Concentration-response effects of ACh and pilocarpine on AQP5 in the APM. A, rat parotid tissue slices were incubated in the absence (lane 1) or presence of 0.01, 0.1, 1, and 10 μM (lanes 2–5, respectively) ACh plus 1 μM eserine or 1 μM eserine (lane 6) for 0.25 min at 37°C, after which APM (5 μg of protein) fractions were prepared and subjected to immunoblot analysis with antibodies to AQP5. B, rat parotid tissue slices were incubated in the absence (lane 1) or the presence of 0.01, 0.1, 1, and 10 μM (lanes 2–5, respectively) pilocarpine for 3 min at 37°C, after which APM (5 μg of protein) fractions were prepared and subjected to immunoblot analysis with antibodies to AQP5. C, AQP5 was purified as described under *Experimental Procedures* and 0.1 μg of protein was subjected to immunoblot analysis with antibodies to AQP5 (lane 1) or with antibodies to AQP5 that were preadsorbed with excess immunizing peptide (lane 2). Profile of enhanced chemiluminescent protein molecular mass markers are shown in lane 3. D, Immunoblots were subjected to densitometric analysis, and the amount of AQP5 in APM, based on the intensity of the chemiluminescence signal, was expressed as a percentage of the value for control tissue. ACh (10 μM) plus 1 μM eserine (○) or 10 μM pilocarpine (●). Data are means ± SE of five independent experiments. ⋆⋆⋆, $p < 0.001$; ⋆⋆, $p < 0.01$; and ⋆, $p < 0.1$ versus the value for control cells.

fmol/mg of protein). SIN-1 and SNAP also induced a 2.5-fold increase of AQP5 in the APM (Figs. 4 and 5). These results suggested that NO donors increase AQP5 levels in the APM by increasing the intracellular concentration of NO.

Effect of ACh on NOS Activity in Isolated Parotid Acinar Cells. Neuronal-type NO activity depends on Ca^{2+} and CaM. Thus, increased $[Ca^{2+}]_i$ caused by activation of mAChRs results in a marked increase in NOS activity (Bredt and Snyder, 1994). It is not clear, however, whether there is endogenous NOS in parotid acinar cells. Rat parotid tissue slices consist of acinar cells, nerve endings, blood vessels, etc., in which different NOS isoforms are present. To obtain direct evidence for NO production in the cells in response to stimulation with ACh in real time, we isolated the acinar cells from rat parotid tissues. The fluorescent NO indicator DAF-2/DA was used to investigate whether rat isolated parotid acinar cells possess endogenous NOS activity. The cells were preloaded with 10 μM DAF-2/DA and then challenged with 10 μM or 0.1 μM ACh plus 1 μM eserine. ACh-stimulation of parotid acinar cells preloaded with DAF-2/DA increased DAF-2 fluorescence in a concentration-dependent manner corresponding to an increase in NO production in the cells (Fig. 6, a and b). When cells suspended in Ca^{2+}-free KRT solution were stimulated with 10 μM ACh, an initial rise in NOS was detected (Fig. 6c). This rise was not maintained for more than 1 min. Stimulation of the isolated cells with 10 μM ACh in the presence of 50 μM BAPTA-AM did not induce an increase in DAF-2 fluorescence (Fig. 6d). This result demonstrates that NOS is present in rat parotid acinar cells and that NOS activity is enhanced by stimulation with ACh.

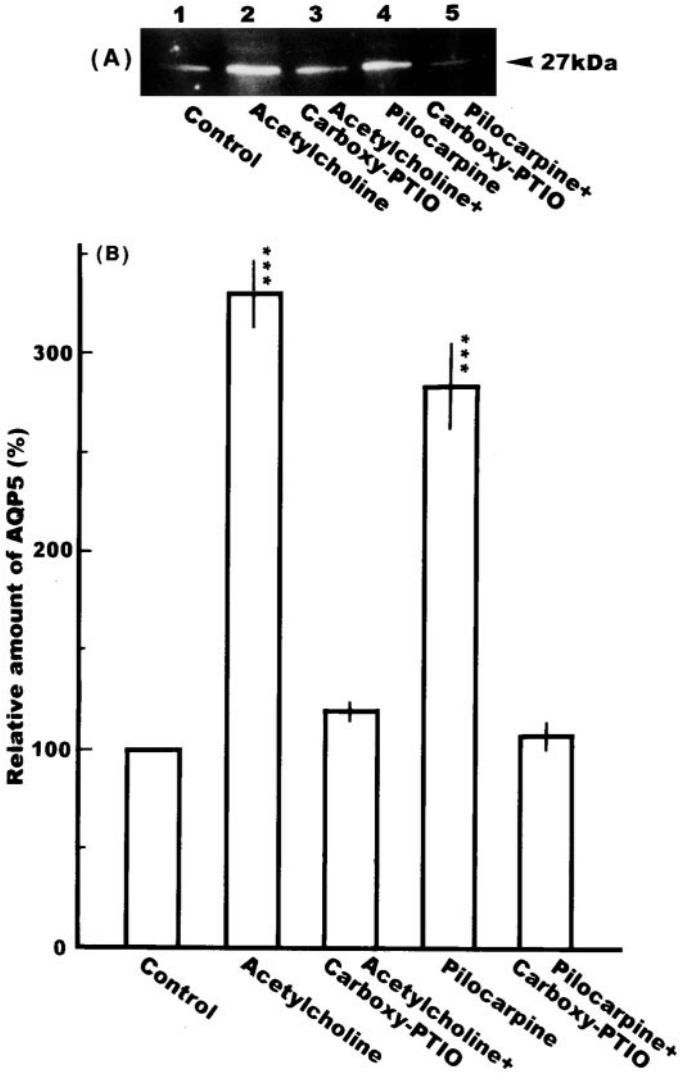

Fig. 3. Effects of carboxy-PTIO on the ACh- and pilocarpine-induced increases in AQP5 levels in the APM of rat parotid glands. A, rat parotid tissue slices were preincubated for 10 min at 37°C in the absence (lanes 1, 2, and 4) or presence (lanes 3 and 5) of 10 μM carboxy-PTIO, and then incubated with 10 μM ACh (lanes 2 and 3) for 0.25 min at 37°C or with 10 μM pilocarpine (lanes 4 and 5) for 3 min at 37°C. The APM fraction (5 μg of protein) was then prepared and subjected to immunoblot analysis with antibodies to AQP5. B, immunoblots similar to those shown in A were subjected to densitometric analysis, and the amount of AQP5 was expressed as a percentage of the value for control cells. Data are means ± SE of three independent experiments. ⋆⋆⋆, $p < 0.001$ versus the value for control cells.

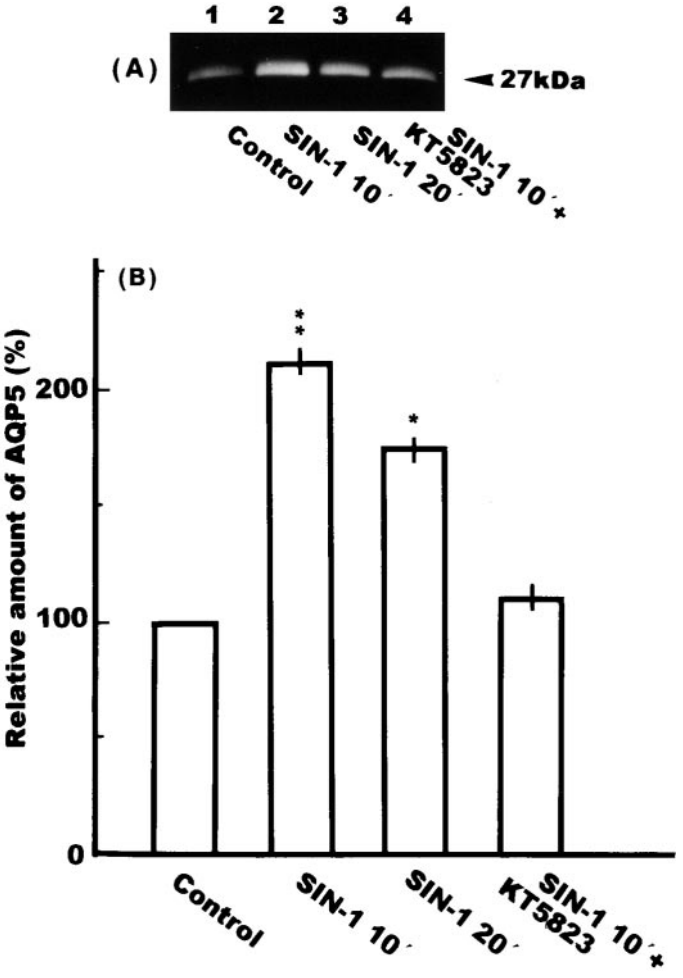

Fig. 4. Effects of SIN-1 on the amounts of AQP5 in the APM, and KT5823 on the SIN-1-induced increase in AQP5 in the APM. A, rat parotid tissue slices were pretreated for 10 min at 37°C in the absence (lanes 1 to 3) or presence (lane 4) of 10 μM KT5823 and then incubated at 37°C in presence of 1 mM SIN-1 for 10 min (lanes 2 and 4) or 20 min (lane 3). The APM fraction (5 μg of protein) was then prepared and subjected to immunoblot analysis with antibodies to AQP5. B, immunoblots similar to those shown in A were subjected to densitometric analysis, and the amount of AQP5 was expressed as a percentage of the value for cells incubated in the absence of SIN-1 and KT5823. Data are means ± S.E. of three independent experiments. ⋆⋆, $p < 0.01$; ⋆, $p < 0.05$ versus the value for control cells.

Effect of PKG on the Amount of AQP5 in the APM. To determine whether the effect of NO is caused by activation of the cGMP signaling pathway, we investigated the effect of KT5823, a specific PKG inhibitor, on the pilocarpine- or NO donor-induced increase of AQP5 in the APM. KT5823 (10 μM) inhibited the pilocarpine-induced activation of PKG (none, 5.98 ± 0.21; KRT5823, 5.24 ± 0.05; pilocarpine, 9.85 ± 0.31; pilocarpine plus KT5823, 5.75 ± 0.28 pmol/mg of protein) in parotid tissues. Pretreatment of the tissues for 10 min with KT5823 inhibited the increase in AQP5 levels in the APM induced by pilocarpine (Fig. 7), SIN-1 (Fig. 4), or SNAP (Fig. 5), indicating that cGMP signaling contributes to the increase of AQP5 in the APM in rat parotid tissues.

Role of CaM-Dependent Enzymes in Both ACh- and Pilocarpine-Induced Increases in AQP5 Levels in the APM. To investigate the mechanisms by which the elevation of $[Ca^{2+}]_i$ increases AQP5 levels in the APM, we examined the roles of CaM-dependent enzymes, CaM kinase II, NOS, and MLCK. First, we examined the possible role of CaM kinase II. KN-62 (10 μM), a selective CaM kinase II inhibitor, inhibited CaM kinase activity (none, 99 ± 8; KN-62, 95 ± 7; pilocarpine, 145 ± 11; pilocarpine plus KN-62, 102 ± 9 nmol/min/mg of protein). Treatment of parotid tissue for 10 min with KN-62 completely blocked the pilocarpine-induced increase of AQP5 in the APM (Fig. 8). This result suggests that the activation of CaM kinase II contributes to the Ca^{2+}-mediated responses to pilocarpine.

Next, to examine the possible role of NOS in ACh- and pilocarpine-induced increases in AQP5 levels, we treated the parotid tissue with 10 μM L-NIL, an NOS inhibitor. This agent inhibited the ACh-induced increases of AQP5 levels in the APM (Fig. 9), suggesting that NOS activation is important for this induction.

MLCK was identified in parotid glands and is known to regulate capacitative Ca^{2+} entry (Kealey and Randle, 1984). To examine the possible role of MLCK in increases of AQP5 levels, we treated parotid tissue with 20 μM ML-9, an MLCK inhibitor. The phosphorylation of MLC under control condition was 28.3 ± 0.9% of the maximum. The MLC phosphorylating activity was 53.8 ± 2.5 and 45.6 ± 0.9% in the tissues incubated with ACh and pilocarpine, respectively. In the presence of ML-9, the activity decreased to 30.3 ± 1.8 and 25.8 ± 1.2%, respectively. Pretreatment with ML-9 inhibited ACh- and pilocarpine-induced increases of AQP5 in the APM (Fig. 10), indicating that MLCK contributes to the increase in AQP5 levels in the APM in rat parotid cells.

Collectively, these data indicate that Ca^{2+} signaling triggered by ACh and pilocarpine results in increases of AQP5 in

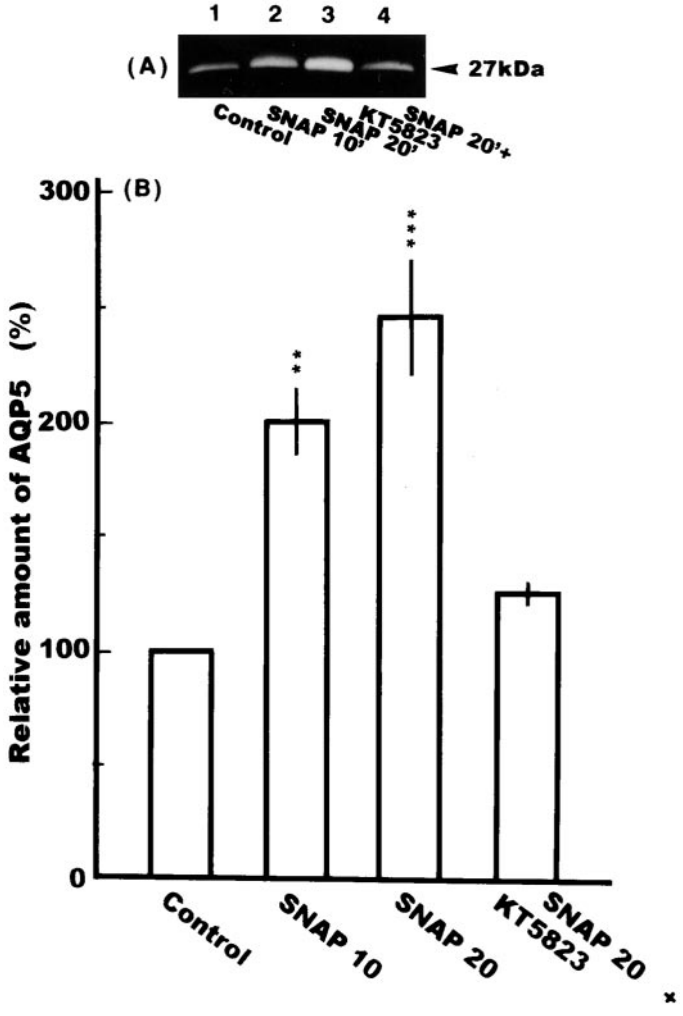

Fig. 5. Effects of SNAP on the amounts of AQP5 in the APM, and KT5823 on the SNAP-induced increase in AQP5 in the APM. A, rat parotid tissue slices were pretreated for 10 min at 37°C in the absence (lanes 1 to 3) or presence (lane 4) of 10 μM KT5823 and then incubated at 37°C in presence of 1 mM SNAP for 10 min (lanes 2 and 4) or for 20 min (lane 3). The APM fraction (5 μg of protein) was then prepared and subjected to immunoblot analysis with antibodies to AQP5. B, immunoblots similar to those shown in A were subjected to densitometric analysis, and the amount of AQP5 was expressed as a percentage of the value for cells incubated in the absence of SNAP and KT5823. Data are means ± S.E. of three independent experiments. ★★★, $p < 0.001$; ★★, $p < 0.01$ versus the value for control cells.

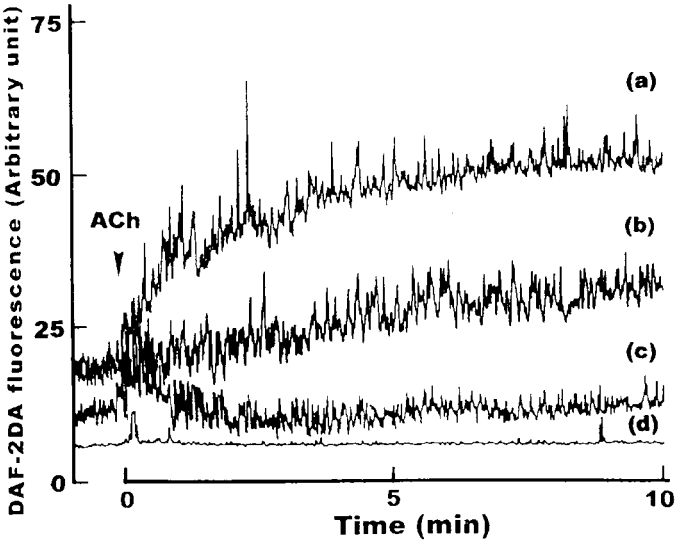

Fig. 6. Effect of ACh on NOS activity in rat parotid acinar cells. NOS activity was measured as changes in fluorescence intensity in isolated parotid acinar cells of rat that were preincubated with 10 μM DAF-2/DA for 30 min. Cells that had been incubated with KRT solution for 10 min were incubated with 10 μM (a) or 0.1 μM ACh in the presence of KRT solution (b). Cells that had been incubated with Ca^{2+}-free KRT solution for 10 min were incubated with 10 μM ACh in the continuous presence of Ca^{2+}-free KRT solution (c). Cells which had been incubated with 50 μM BAPTA/AM for 10 min were incubated with 10 μM ACh in the continuous presence of BAPTA/AM (d). The traces are representative of three to five independent experiments. Arrow, application of ACh.

the APM via activation of CaM-dependent enzymes, CaM kinase II, NOS, and MLCK.

Effects of c-AMP and c-GMP on AQP5 Levels in the APM. NO increases cGMP formation via stimulation of GC. To investigate the effect of cGMP on AQP5 levels in the APM, tissues were incubated with 10 μM dbcGMP and 10 μM dbcAMP for 10 min. The incubation of dbcGMP, but not dbcAMP, induced an increase in AQP5 in the APM of rat parotid glands (Fig. 11). In the presence of BAPTA-AM, treatment of the tissues with dbcGMP did not increase AQP5 in the APM. These results demonstrate that cGMP accumulation in rat parotid acinar cells induces the increase in AQP5 in the APM in the presence of Ca^{2+}.

Effect of Ca^{2+}-Free KRT Solution on the ACh-Induced Increase in the AQP5 in the APM. To determine whether Ca^{2+} released from intracellular storage sites or the entry of extracellular Ca^{2+} into cells contributes to the increase in AQP5 in the APM, we measured the ACh-induced increase in AQP5 in the APM of parotid tissues incubated with Ca^{2+}-free KRT solution to remove the effect of extracellular Ca^{2+}. In a Ca^{2+}-free KRT solution, ACh induced a 2.4-fold increase in the amount of AQP5 in the APM (Fig. 12). With Ca^{2+} in the KRT solution, however, ACh induced a 3.8-fold increase (Fig. 1). Although ACh induces an increase

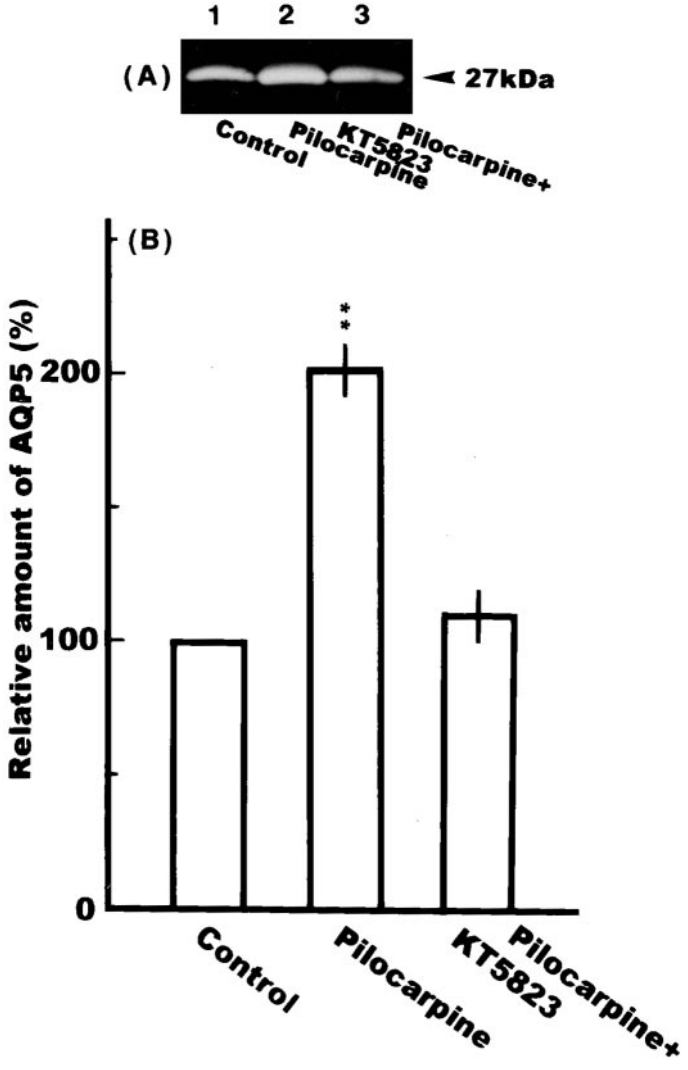

Fig. 7. Effect of KT5823 on the pilocarpine-induced increase in AQP5 in the APM. A, rat parotid tissue slices were pretreated for 10 min at 37°C in the absence (lanes 1 and 2) or presence of 10 μM KT5823 (lane 3) and then incubated for 3 min at 37°C in the absence (lane 1) or presence (lanes 2 and 3) of 10 μM pilocarpine in the continuous absence or presence of KT5823. The APM fraction (5 μg of protein) was then prepared and subjected to immunoblot analysis with antibodies to AQP5. B, immunoblots similar to those shown in A were subjected to densitometric analysis, and the amount of AQP5 was expressed as a percentage of the value for cells incubated in the absence of pilocarpine and KT5823. Data are means ± S.E. of three independent experiments. **, $p < 0.01$ versus the value for control cells.

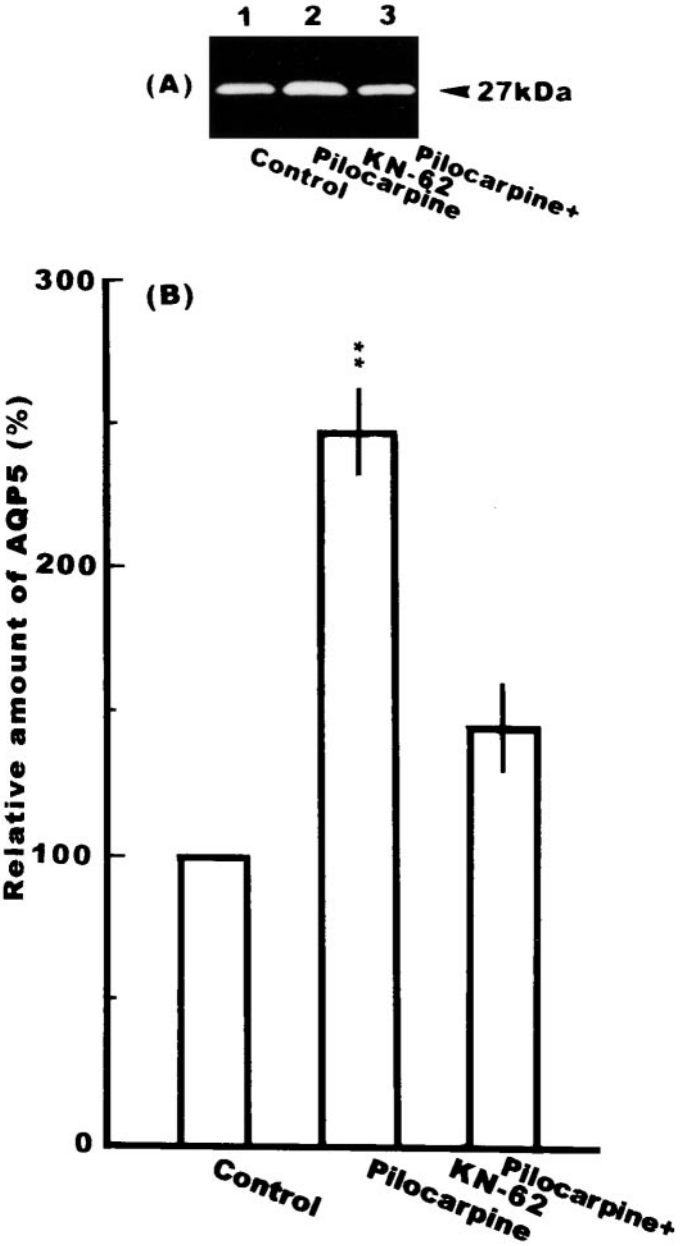

Fig. 8. Effect of KN-62 on the pilocarpine-induced increase in AQP5 in the APM. A, rat parotid tissue slices were pretreated for 10 min at 37°C in the absence (lanes 1 and 2) or presence of 10 μM KN-62 (lane 3) and then incubated for 3 min at 37°C in presence of 10 μM pilocarpine (lanes 2 and 3). The APM fraction (5 μg of protein) was then prepared and subjected to immunoblot analysis with antibodies to AQP5. B, immunoblots similar to those shown in A were subjected to densitometric analysis, and the amount of AQP5 was expressed as a percentage of the value for cells incubated in the absence of pilocarpine and KN-62. Data are means ± SE of three independent experiments. **, $p < 0.01$ versus the value for control cells.

in AQP5 in the APM via Ca^{2+} release from intracellular storage sites, these data indicated that the maximal effect of ACh was in the presence of Ca^{2+} entry into cells. Thus, both the Ca^{2+} release from intracellular storage sites and the entry of Ca^{2+} into cells regulate the amount of AQP5 in the APM.

Effects of Several Inhibitors on AQP5 Levels in the APM of Nonstimulated Parotid Tissues. In the above experiments, tissues incubated with mAChR agonists or NO donors were used to investigate the effect of NO/cGMP signal transduction on AQP5 levels in the APM of excited parotid tissues. Next, we investigated the effect of NO/cGMP signal transduction on AQP5 levels in the APM of nonstimulated parotid tissues (Fig. 13). Carboxy-PTIO at the concentration that inhibited ACh- or pilocarpine-induced increases in AQP5 in the APM (Fig. 3) had no significant effect on the AQP5 levels in the APM (Fig. 13A, lane 2), suggesting that NO generated after mAChR-stimulation of parotid cells increases the AQP5 levels in the APM. KT5823, at the concentration that inhibited the SIN-1–, SNAP-, or pilocarpine-induced increases in AQP5 levels in the APM (Figs. 4, 5, and 7), had no significant effect on the AQP5 levels in the APM (Fig. 13A, lane 3), suggesting that PKG activated after the stimulation of NO generation increases the AQP5 levels in the APM. IBMX, at the concentration that inhibited cGMP

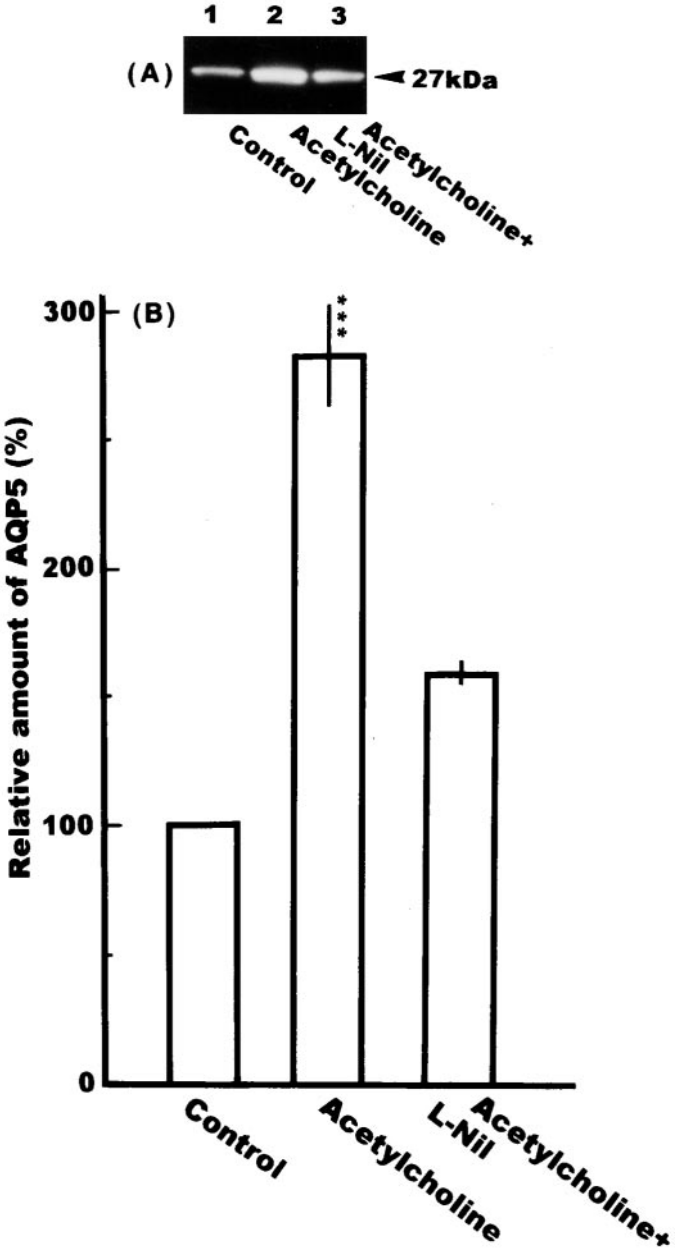

Fig. 9. Effects of L-NIL on the ACh-induced increase in AQP5 in the APM. A, rat parotid tissue slices were pretreated for 10 min at 37°C in the absence (lanes 1 and 2) or presence of 10 μM L-NIL (lane 3) and then incubated for 0.25 min at 37°C in presence of 10 μM ACh (lanes 2 and 3). The APM fraction (5 μg of protein) was then prepared and subjected to immunoblot analysis with antibodies to AQP5. B, immunoblots similar to those shown in A were subjected to densitometric analysis, and the amount of AQP5 was expressed as a percentage of the value for cells incubated in the absence of ACh and L-Nil. Data are means ± SE of three independent experiments. ⋆⋆⋆, $p < 0.001$ versus the value for control cells.

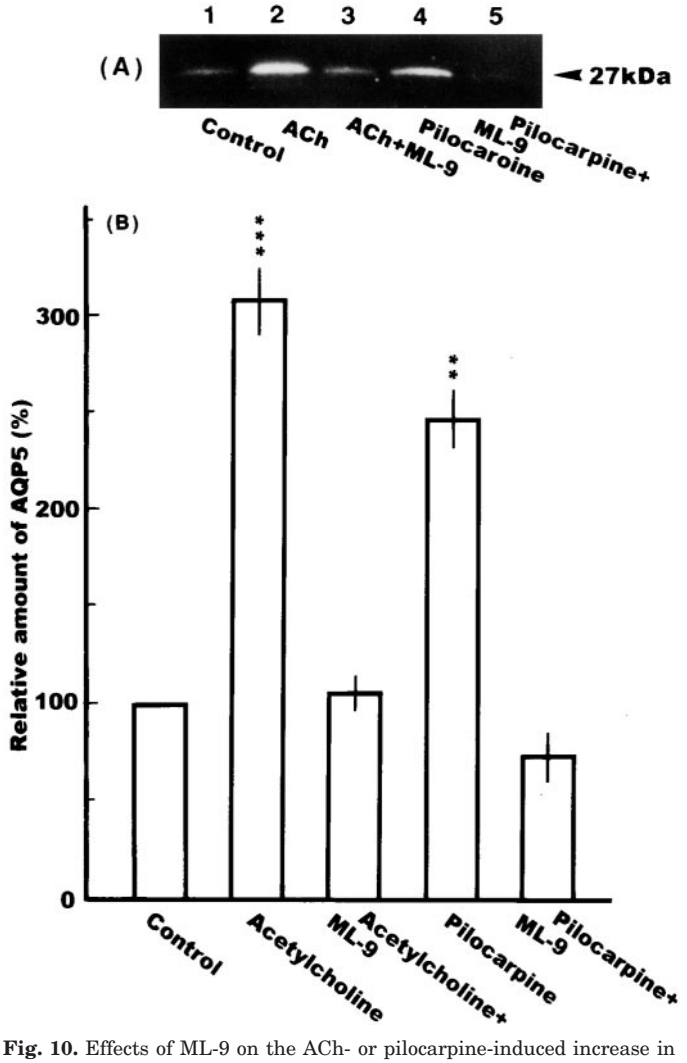

Fig. 10. Effects of ML-9 on the ACh- or pilocarpine-induced increase in AQP5 in the APM. A, rat parotid tissue slices were pretreated for 10 min at 37°C in the absence (lanes 1, 2, and 4) or presence of 20 μM ML-9 (lanes 3 and 5) and then incubated for 0.25 min at 37°C in presence of 10 μM ACh (lanes 2 and 3) or for 3 min at 37°C in presence of 10 μM pilocarpine (lanes 4 and 5). The APM fraction (5 μg of protein) was then prepared and subjected to immunoblot analysis with antibodies to AQP5. B, immunoblots similar to those shown in A were subjected to densitometric analysis, and the amount of AQP5 was expressed as a percentage of the value for cells incubated in the absence of ACh, pilocarpine, and ML-9. Data are means ± S.E. of three independent experiments. ⋆⋆⋆, $P < 0.001$; ⋆⋆, $p < 0.01$ versus the value for control cells.

phosphodiesterase activity, did not affect AQP5 levels in the APM (Fig. 13B, lane 2). KN-62, L-NIL, and ML-9 at the concentrations that inhibited ACh- or pilocarpine-induced increases in AQP5 levels in the APM (Figs. 8–10), had no significant effects on the AQP5 levels in the APM (Fig. 13, B, lanes 3–5). These results demonstrate that at the concentrations indicated in legends of Fig. 13, the NO/cGMP signal transduction inhibitors do not affect AQP5 levels in the APM in nonexcited parotid tissues.

Effects of ACh or dbcGMP on the $[Ca^{2+}]_i$ in Isolated Parotid Acinar Cells. $[Ca^{2+}]_i$ was measured in isolated parotid acinar cells loaded with fura-2/AM to demonstrate whether the elevation of AQP5 levels in the APM coincided with the elevation of $[Ca^{2+}]_i$. $[Ca^{2+}]_i$ rapidly increased in a concentration-dependent manner after exposure of the isolated parotid acinar cells to ACh (Fig. 14A). Exposure of parotid tissue for 0.25 min to 10 μM ACh induced 10-fold increases in the cGMP concentration (none, 26.7 ± 2.3; 10 μM ACh, 283.4 ± 10.9; 0.1 μM, 123.8 ± 8.9 fmol/mg of protein). Stimulation of the isolated cells with 10 μM ACh in the presence of 50 μM BAPTA-AM did not induce an increase in cGMP (22.5 ± 2.1 fmol/mg of protein) or in fura-2 fluorescence. These data indicate that cGMP production is related to the elevation of $[Ca^{2+}]_i$ and NO generation. $[Ca^{2+}]_i$ was then measured at successive time points after exposure of isolated parotid acinar cells to 10 or 0.1 μM dbcGMP. $[Ca^{2+}]_i$ increased gradually (Fig. 14B), consistent with a previous report by Mathes and Thompson (1996). The enhancement of $[Ca^{2+}]_i$ in isolated parotid acinar cells after adding dbcGMP was inhibited by the presence of KT5823 (Fig. 14B). These results suggest that the stimulation of mAChR makes Ca^{2+} homeostasis via activation of NO/cGMP signal transduction.

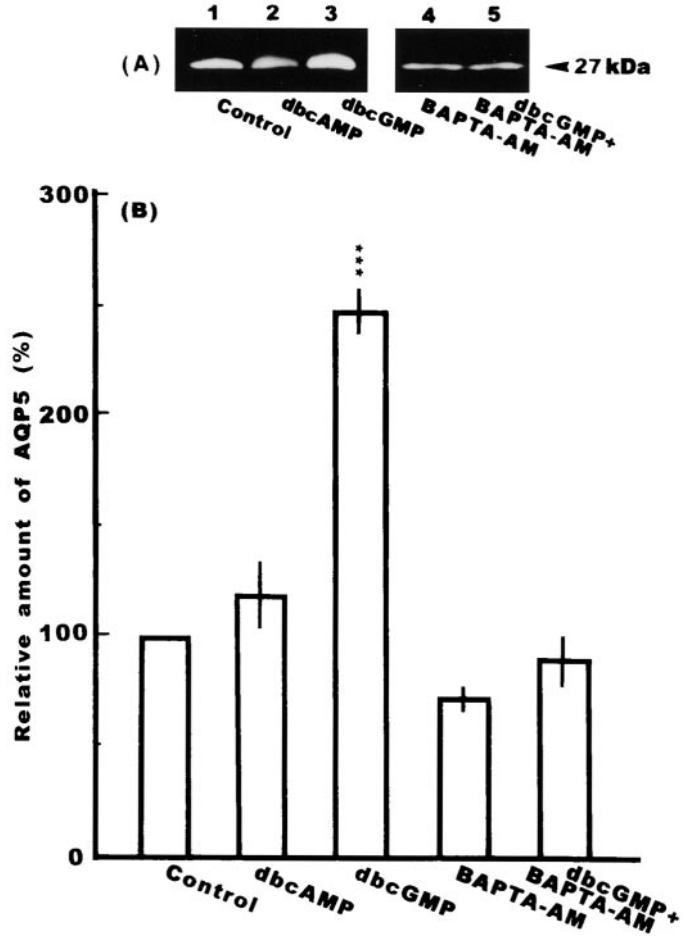

Fig. 11. Effects of dbcGMP on the amounts of AQP5 in the APM, and BAPTA on the dbcGMP-induced increases in AQP5 in the APM. A, rat parotid tissue slices were pretreated for 10 min at 37°C in the absence (lanes 1 to 3) or presence of 50 μM BAPTA-AM (lanes 4 and 5) and then incubated for 10 min at 37°C in presence of 10 μM dbcAMP (lane 2) or dbcGMP for 10 min (lanes 3 and 5). The APM fraction (5 μg of protein) was then prepared and subjected to immunoblot analysis with antibodies to AQP5. B, immunoblots similar to those shown in A were subjected to densitometric analysis, and the amount of AQP5 was expressed as a percentage of the value for cells incubated in the absence of dbcGMP and BAPTA-AM. Data are means ± S.E. of three independent experiments. ⋆⋆ $p < 0.01$ versus the value for control cells.

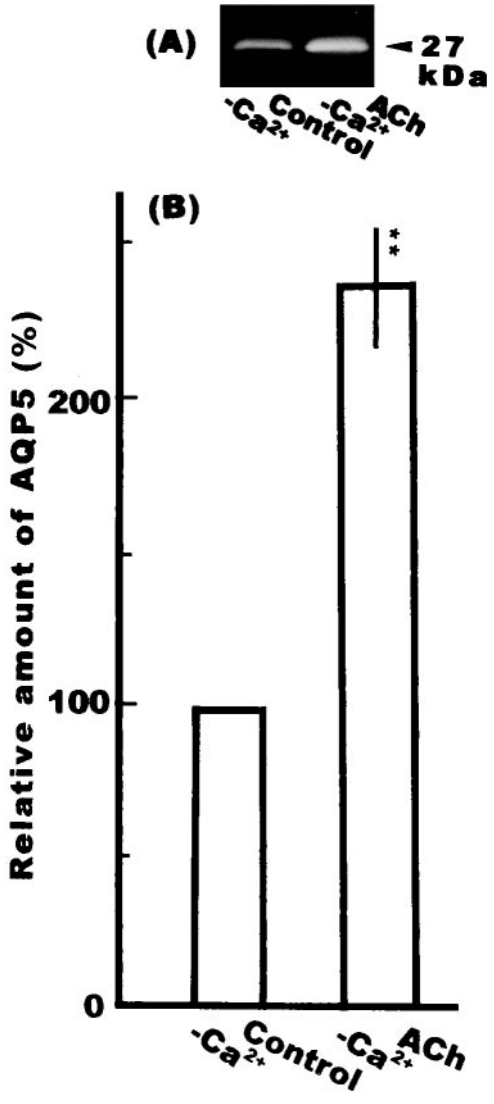

Fig. 12. Effect of Ca^{2+}-free KRT solution on the amounts of AQP5 in the APM. A, rat parotid tissue slices were incubated with Ca^{2+}-free KRT solution in the absence (left lane) or presence (right lane) of 10 μM ACh plus 1 μM eserine for 0.25 min at 37°C. APM (5 μg of protein) fractions were prepared and subjected to immunoblot analysis with antibodies to AQP5. B, immunoblots were subjected to densitometric analysis, and the amount of AQP5 in each fraction, based on the intensity of the chemiluminescence signal, was expressed as a percentage of the value for control tissue. Data are means ± S.E. of three independent experiments. ⋆⋆, $p < 0.01$ versus the value for control cells.

Discussion

Rat parotid glands express M_2 and M_3 mAChRs; the M_3 mAChRs represent 90% of the total number of precipitable mAChRs (Ehlert et al., 1996). As shown in Fig. 1, M_3 mAChR activation by ACh or pilocarpine increases AQP5 levels in the APM of rat parotid cells. The M_3 mAChR-stimulated increases of AQP5 in the APM was inhibited by treatment of the tissues with U73122, TMB-8, and dantrolene (Ishikawa et al., 2000), indicating that M_3 mAChRs activate PLC, increase the release of Ca^{2+} via the activation of IP_3 and ryanodine receptors, and induce an increase in AQP5 levels in the APM. M3 mAChR stimulation also induces the generation of DAG and leads to PKC activation. The M_3 mAChR-stimulated increase of AQP5 in the APM, however, was not inhibited by treatment with GF 109203X (Ishikawa et al., 2000), indicating that PKC did not regulate the amount of AQP5 in the APM. Intracellular Ca^{2+}-dependent cellular process are regulated by the ubiquitous Ca^{2+} -binding protein, CaM, which activates CaM-dependent protein kinase I, II, III, and MLCK (Stull, 2001; Soderling et al., 2001). Also, increased $[Ca^{2+}]_i$ results in markedly increased NOS activity to form NO from the amino acid L-arginine. NO exerts its biologic effects through the activation of GC and the production of cGMP or through cGMP- independent mechanisms such as nitrosylation (Moncada et al., 1991; Lucas et al., 2000). To investigate the contribution of NO/cGMP signaling to the M_3 mAChR-stimulated increase in AQP5 in the APM of rat parotid cells, rat parotid tissues were treated with carboxy-PTIO, an NO scavenger. Treatment with carboxy-PTIO inhibited ACh- or pilocarpine-induced increases in AQP5 in the APM (Fig. 3). On the other hand, parotid tissues treated with the NO-releasing compounds SIN-1 and SNAP alone had increased levels of AQP5 in the APM (Fig. 4 and 5). These results indicate that NO works as a postsynaptic intracellular messenger to induce an increase in AQP5 levels in the APM.

In general, NO activates GC, which produces cGMP that then activates PKG (Moncada et al., 1991; Lucas et al., 2000). The selective PKG inhibitor KT5823 blocked SIN-1-, SNAP-, and pilocarpine-induced increases of AQP5 in the APM (Figs. 4, 5, and 7). Furthermore, treatment with dbcGMP increased AQP5 levels in the APM (Fig. 11). In fact, treatment of the tissues with SIN-1 or SNAP remarkably induced cGMP accumulation and induced amylase secretion from the parotid glands, suggesting that NO activates GC and produces cGMP in parotid tissues. The results of the present study indicate that NO increases AQP5 in the APM via activation of PKG in rat parotid cells (Figs. 4, 5, and 7).

NO production is reported to occur in neurons and macrophages, etc. (Moncada et al., 1991). In parotid glands, however, it was not clear whether NO produced in neurons and endothelial cells diffuses to parotid acinar cells or if NO is endogenously synthesized in parotid acinar cells. Using an NO indicator, DAF-2/DA, we demonstrated that endogenous NOS was present in parotid acinar cells and activated by the increase in $[Ca^{2+}]_i$ induced by the ACh stimulation of M_3 $mAChR_3$ (Fig. 6). Treatment of the tissues with L-NIL, a NOS inhibitor, blocked the ACh-induced increase of AQP5 in the APM (Fig. 9), consistent with the presence of NOS in parotid tissues.

Pretreatment of the tissues with KN-62, a specific CaM kinase II inhibitor, or ML-9, a specific MLCK inhibitor, inhibited ACh- or pilocarpine-induced increases of AQP5 in the APM (Figs. 8 and 10). CaM kinase II and MLCK have multiple functions (Kamm and Stull, 2001; Soderling et al., 2001). In pancreatic cells, the effect of Ca^{2+} on exocytosis is mediated by activation of CaM kinase II (Gromada et al., 1999) and granule movements are dependent on activation of Ca^{2+}/CaM dependent phosphorylation of MLC (Niwa et al., 1998). In Ca^{2+} homeostasis, CaM kinase II senses cellular Ca^{2+} oscillations (Soderling et al., 2001) and MLCK regulates capacitative Ca^{2+} entry (Watanabe et al., 1998).

NO has multiple functions, which include acting as an important messenger and having profound effects on Ca^{2+} homeostasis. NO regulates Ca^{2+} homeostasis at many sites involved in voltage-dependent Ca^{2+} channels and voltage-independent, store-operated Ca^{2+} channels, modulation of

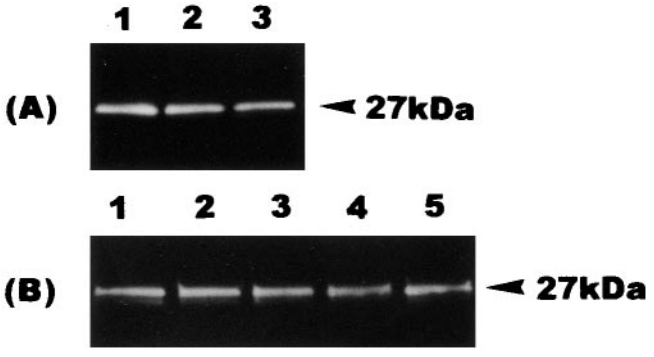

Fig. 13. Effects of carboxy-PTIO, KT5823, IBMX, KN-62, L-NIL, and ML-9 on AQP5 levels in the APM of nonstimulated parotid tissues. A, rat parotid tissue slices were incubated for 20 min at 37°C in the absence (lane 1) or presence of 10 μM carboxy-PTIO (lane 2) and 10 μM KT5823 (lane 3). B, rat parotid tissue slices were incubated for 20 min at 37°C in the absence (lane 1) or presence of 0.5 mM IBMX (lane 2), 10 μM KN-62 (lane 3), 10 μM L-NIL (lane 4), and 20 μM ML-9 (lane 5). The APM fraction (5 μg of protein) was then prepared and subjected to immunoblot analysis with antibodies to AQP5.

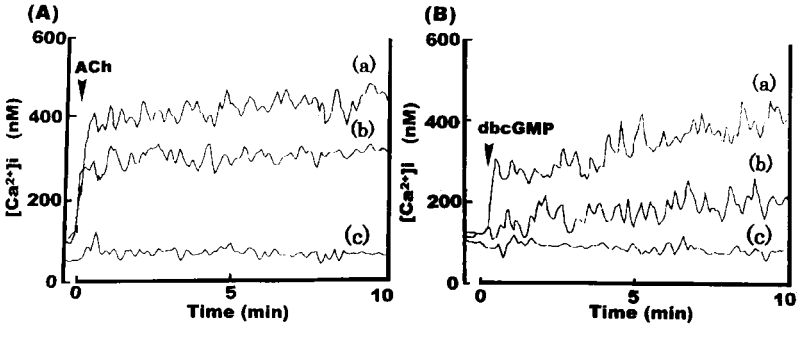

Fig. 14. Effects of ACh and dbcGMP on $[Ca^{2+}]_i$ in isolated parotid acinar cells. The $[Ca^{2+}]_i$ was measured as changes in fluorescence intensity in isolated rat parotid acinar cells that were preincubated with fura-2/AM. A, cells that had been incubated with (c) or without (a and b) 50 μM BAPTA/AM for 10 min were incubated with 10 μM (a and c) or 0.1 μM ACh (b). B, cells that had been incubated with (c) or without (a and b) 10 μM KT5823 for 10 min were incubated with 10 μM (a and c) or 0.1 μM dbcGMP. The traces are representative of three independent experiments. Arrow, application of ACh and dbcGMP.

IP_3-induced intracellular Ca^{2+} release, Ca^{2+} release from ryanodine stores, regulation of Ca^{2+} influx, IP_3, and cADP-ribose generation (Clementi, 1998). The principal targets of cGMP are phosphodiesterase, resulting in interference with the cAMP-signaling pathway; cGMP-gated channels, such as AQP1 (Anthony et al., 2000); PKGs; and cADP-ribose-dependent Ca^{2+} channels (Willmott et al., 1996; Looms et al., 2001). Treatment with dbcGMP alone increases AQP5 levels in the APM (Fig. 11). Preventing the elevation of $[Ca^{2+}]_i$ with BAPTA-AM, however, inhibited dbcGMP-induced increases of AQP5 in the APM (Fig. 11). Thus, the NO/cGMP signaling pathway regulates the amount of AQP5 in the APM via the elevation of $[Ca^{2+}]_i$.

ACh and dbcGMP increased the $[Ca^{2+}]_i$ in rat parotid acinar cells (Fig. 14). Mathes and Thompson (1996) demonstrated that mAChR-activation stimulated NOS, which enhances cGMP production and greater Ca^{2+} influx in neuroblastoma. Xu et al. (1997) also reported that nNOS activated by Ca^{2+} release from intracellular stores generated cGMP and regulated Ca^{2+} influx in rat pancreatic and submandibular salivary glands. Watson et al. (1999) and Looms et al. (2001) demonstrated that mAChR activation stimulates Ca^{2+}-dependent NOS, leading to the production of NO and the release of Ca^{2+} from ryanodine-sensitive stores. To determine whether the enhancement of $[Ca^{2+}]_i$ is caused by the Ca^{2+} release from intracellular storage sites or by the entry of extracellular Ca^{2+} into cells, we measured the ACh-induced increase in AQP5 levels in the APM of parotid tissues incubated with Ca^{2+}-free KRT solution. In the absence of extracellular Ca^{2+}, ACh induced a 2.4-fold increase in AQP5 in the APM (Fig. 12). In the presence of extracellular Ca^{2+}, however, ACh induced a 3.8-fold increase (Fig. 1). Although ACh induces an increase in AQP5 in the APM via the Ca^{2+} release from intracellular stores, these data indicate that the maximum effect of ACh occurs with Ca^{2+} entry into cells. In addition, ML-9 (Fig. 10) or dantrolene (Ishikawa et al., 2000) inhibited ACh- or epinephrine-induced increases in the AQP5 levels in the APM, respectively, suggesting that both Ca^{2+} release from intracellular stores and Ca^{2+} entry on plasma membranes regulates the AQP5 levels in the APM. Taken together, both the Ca^{2+} release from intracellular stores and the entry of Ca^{2+} into cells regulate the amount of AQP5 in the APM. In our experiments, it is not clear that this elevated $[Ca^{2+}]_i$ depends on Ca^{2+} release from intracellular stores or Ca^{2+} entry via voltage-independent channels on plasma membranes. It is clear that NO/cGMP signal transduction is involved in $[Ca^{2+}]_i$ homeostasis in rat parotid acinar cells.

As reported previously, ACh and epinephrine stimulate an increase in AQP5 levels in the APM by movement of cytosolic components (Ishikawa et al., 1999, 2000). The mechanism underlying the insertion of the recruitment membrane into the plasma membrane, which is regulated by Ca^{2+}, has attracted much attention (Barroso et al., 1996). In the present study, NO/cGMP signal transduction after activation of M_3 mAChRs contributed to increased levels of AQP5 in the APM in rat parotid glands. These results indicate that enhancement of $[Ca^{2+}]_i$ fulfills a crucial role in ACh- and pilocarpine-induced increases of AQP5 in the APM of rat parotid acinar cells.

Acknowledgments

We thank Yumiko Yoshinaga for assistance in preparing the manuscript.

References

Anthony TL, Brooks HL, Boassa D, Leonov S, Yanochko GM, Regan JW, and Yool AJ (2000) Cloned human aquaporin-1 is a cyclic GMP-gated ion channel. *Mol Pharmacol* **57:**576–588.

Barroso MR, Bernd KK, DeWitt ND, Chang A, Mills K, and Sztul ES (1996) A novel Ca^{2+} -binding protein, p22, is required for constitutive membrane traffic. *J Biol Chem* **271:**10183–10187.

Baum BJ (1993) Principle of saliva secretion. *Ann NY Acad Sci* **694:**17–23.

Bouley R, Breton S, Sun T-X, McLaughlin M, Nsumu NN, Lin HY, Ausiello DA, and Brown D (2000) Nitric oxide and atrial natriuretic factor stimulate cGMP-dependent membrane insertion of aquaporin 2 in renal epithelial cells. *J Clin Invest* **106:**1115–1126.

Bredt DS and Snyder SH (1994) Nitric oxide: a physiologic messenger molecule. *Annu Rev Biochem* **63:**175–195.

Clementi E (1998) Role of nitric oxide and its intracellular signaling pathways in the control of Ca^{2+} homeostasis. *Biochem Pharmacol* **55:**713–718.

Dijulio DH, Watson EL, Pessah IN, Jacobson KL, Ott SM, Buck ED, and Singh JC (1997) Ryanodine receptor type III (Ry3R) identification in mouse parotid acini. *J Biol Chem* **272:**15687–15696.

Ehlert FJ, Griffin MT, and Glidden PF (1996) The interaction of enantiomers of aceclidine with subtypes of the muscarinic receptor. *J Pharmacol Exp Ther* **279:** 1335–1344.

Gromada J, Hoy M, Renstrom E, Bokvist, Eliasson L, Gopel S, and Rorsman P (1999) CaM kinase II-dependent mobilization of secretory granules underlies acetylcholine-induced stimulation of exocytosis in mouse pancreatic B-cells. *J Physiol* **518:** 745–759.

Hata F, Ishida H, Kagawa K, Kondo E, Kondo S, and Noguchi Y (1983) α-Adrenoceptor alterations coupled with secretory response in rat parotid tissues. *J Physiol* **341:**185–196.

Ishikawa Y, Eguchi T, Skowronski MT, and Ishida H (1998) Acetylcholine acts on M3 muscarinic receptors and induces the translocation of aquaporin 5 water channel via cytosolic Ca^{2+} elevation in rat parotid glands. *Biochem Biophys Res Commun* **245:**835–840.

Ishikawa Y, Eguchi T, Skowronski MT, and Ishida H (1999) α1-Adrenoceptor-induced trafficking of aquaporin-5 to the apical plasma membrane of rat parotid cells. *Biochem Biophys Res Commun* **265:**94–100.

Ishikawa Y, Skowronski MT, and Ishida H (2000) Persistent increase in the amount of aquaporin-5 in the apical plasma membrane of rat parotid acinar cells induced by a muscarinic agonist SNI-2011. *FEBS Lett* **477:**253–257.

Jansen A, Osborne JA, Brown R, Loscalzo J, and Stanler JS (1992) The relaxant properties in guinea pig airways of *S*-nitrosothiols. *J Pharmacol Exp Ther* **261:** 154–160.

Kankaanranta H, Knowles RG, Vuorinen P, Kosonen O, Holm P and Moilanen E (1997) 3-Morpholino-sydnonimine-induced suppression of human neutrophil degranulation is not mediated by cyclic GMP, nitric oxide or peroxynitrite: inhibition of the increase in intracellular free calcium concentration by *N*-morpholino-iminoacetonitrile, a metabolite of 3-morpholino-sydnonimine. *Mol Pharmacol* **51:** 882–888.

Kamm KE and Stull JT (2001) Dedicated myosin light chain kinases with diverse cellular functions. *J Biol Chem* **276:**4527–4530.

Kealey T and Randle PJ (1984) Studies on rat parotid-cell actomyosin. *Biochem J* **220:**291–299.

Kim M, Kim S, Kim HS, Chang JW, Hong YS, Kim HW, and Park CS (1998) Regulation of renin secretion through reversible phosphorylation of myosin light chain kinase and protein phosphatase type 1. *J Pharmacol Exp Ther* **285:**968–974.

King LS and Agre P (1996) Pathophysiology of the aquaporin water channels. *Annu Rev Physiol* **58:**619–648.

Krane CM, Melvin JE, Nguyen HV, Richardson L, Towne JE, Doetschmam T, and Menon AG (2001) Salivary acinar cells from aquaporin 5-deficient mice have decreased membrane water permeability and altered cell volume regulation. *J Biol Chem* **276:**23413–23420.

Kumakura K, Sasaki K, Sakura T, Ohara-Imaizumi M, Misonou H, Nakamura S, Matsuda Y, and Nonomura Y (1994) Essential role of myosin light chain kinase in the mechanism for MgATP-dependent priming of exocytosis in adrenal chromaffin cells. *J Neurosci* **14:**7695–7703.

Laemmli K (1970) Clevage of structural proteins during the assembly of the head of bacteriophage T4. *Nature (Lond)* **227:**680–685.

Looms DK, Tritsaris K, Nauntofte B, and Dissing S (2001) Nitric oxide and cGMP activate Ca^{2+}-release processes in rat parotid acinar cells. *Biochem J* **355:**87–95.

Lucas KA, Pitari GM, Kazerounian S, Ruiz-Stewart I, Park J, Schulz S, Chepenik KP, and Waldman SA (2000) Guanylyl cyclases and signaling by cyclic GMP. *Pharmacol Rev* **52:**375–413.

Ma T, Song Y, Gillespie A, Carlson EJ, Epstein CJ, and Verkman AS (1999) Defective secretion of saliva in transgenic mice lacking aquaporin-5 water channels. *J Biol Chem* **274:**20071–20074.

Ma T and Verkman AS (1999) Aquaporin water channels in gastrointestinal physiology. *J Physiol* **517:**317–326.

Mathes C and Thompson SH (1996) The nitric oxide/cGMP pathway couples muscarinic receptors to the activation of Ca^{2+} influx. *J Neurosci* **16:**1702–1709.

Moncada S, Palmer RMJ, and Higgs EA (1991) Nitric oxide: physiology, pathophysiology, and pharmacology. *Pharmacol Rev* **43:**109–142.

Niwa T, Matsukawa Y, Senda T, Nimura Y, Hidaka H, and Niki I (1998) Acetylcholine activates intracellular movements of insulin granules in pancreatic β-cells via inositol trisphosphate-dependent mobilization of intracellular Ca^{2+}. *Diabetes* **47:** 1699–1706.

Paul E, Hurtubise Y, and LeBel D (1992) Purification and characterization of the apical plasma membrane of the rat pancreatic acinar cell. *J Membrane Biol* **127:**129–137.
Putney JWJr (1986) Identification of cellular activation mechanisms associated with salivar secretion. *Annu Rev Physiol* **48:**75–88.
Raina S, Preston GM, Guggino WB, and Agre P (1995) Molecular cloning and characterization of an aquaporin cDNA from salivary, lacrimal and respiratory tissues. *J Biol Chem* **270:**1908–1912.
Soderling TR, Chang B, and Brickey D (2001) Cellular signaling through multifunctional Ca^{2+}/calmodulin-dependent protein kinase II. *J Biol Chem* **276:**3719–3722.
Stull JT (2001) Ca^{2+}-dependent cell signaling through calmodulin-activated protein phosphatase and protein kinases minireview series. *J Biol Chem* **276:**2311–2312.
Tritsaris K, Looms DK, Nauntofte B, and Dissing S (2000) Nitric oxide synthesis causes inositol phosphate production and Ca^{2+} release in rat parotid acinar cells. *Pflueg Arch Eur J Physiol* **440:**223–228.
Turner RJ, George JN, and Baum BJ (1986) Evidence for a $Na^+/K^+/Cl^-$ cotransport system in basolateral membrane vesicles from the rabbit parotid. *J Membrane Biol* **94:**143–152.
Watanabe H, Takahashi R, Zhang XX, Hayashi H, Ando J, Isshiki M, Seto M, Hidaka H, Niki I, and Ohno R (1998) An essential role of myosin light chain kinase in the regulation of agonist- and fluid flow-stimulated Ca^{2+} influx in endothelial cells. *FASEB J* **12:**341–348.
Watson E, Jacobson KL, Singh JC, and Ott SM (1999) Nitric oxide acts independently of cGMP to modulate capacitative Ca^{2+} entry in mouse parotid acini. *Am J Physiol* **277:**C262–C270.
Willmott N, Sethi JK, Walseth TF, Lee HC, White AM, and Calione A (1996) Nitric oxide-induced mobilization of intracellular calcium via the cyclic ADP-ribose signaling pathway. *J Biol Chem* **271:**3699–3705.
Xu X, Zeng W, Diaz J, Lau KS, Gukovskaya AC, Brown RJ, Pandol SJ, and Muallem S (1997) nNOS and Ca^{2+} influx in rat pancreatic acinar and submandibular salivary gland cells. *Cell Calcium* **22:**217–228.

Address correspondence to: Dr. Yasuko Ishikawa, Department of Pharmacology, Tokushima University School of Dentistry, 3–18-15 Kuramoto-cho, Tokushima 770-8504, Japan. E-mail: isikawa@dent.tokushima-u.ac.jp